# Wave-Mud interactions across the
# Louisiana Inner Shelf to the Shoreline

Tim T. Janssen

Theiss Research
La Jolla, California 92037
t: 415 609 5359; f: 877 350 2454; e: ttjanssen@gmail.com

## LONG-TERM GOALS

The wave-driven dynamics of the coastal ocean, which is important for transport processes, mixing and circulation, is strongly affected by mud deposits on the continental shelf and in the nearshore. However, the mechanics of wave-mud interaction and the impacts on coastal wave dynamics is not well understood. The overall objective of this work is to contribute to the understanding of the macro-scale damping effects of mud on waves and to improve modeling and prediction of wave evolution along muddy coastlines.

## OBJECTIVES

The specific objectives of the proposed effort are to: 1) establish a comprehensive dataset from two new datasets acquired in 2008 (ONR-funded wave-mud MURI) of waves propagating across more than 25 km over a muddy seafloor, and 2) determine the characteristics of mud-induced dissipation of wave energy from intermediate- to shallow-water depths.

## APPROACH

To improve our understanding of mud-induced damping rates on surface waves, and its variation across the shelf, we combine observations made during the 2008 MURI field experiment (MUDEX08) by the NPS/SIO and WHOI teams, to establish a comprehensive data set of wave evolution. The high spatial coverage allows a detailed analysis of mud-induced wave damping across the shelf to the shoreline, including the transition to shallow water. The proposed work includes: 1) a detailed analysis of the combined data set to determine damping characteristics across the shelf, and 2) implementation of a conventional third-generation wind-wave model to assess the effects of mud on wave propagation and wind-wave generation, and 3) investigate the role played by nonlinear interactions or other coastal processes in the damping of short waves.

| 1. REPORT DATE **2012** | 2. REPORT TYPE **N/A** | 3. DATES COVERED **-** | |
|---|---|---|---|
| 4. TITLE AND SUBTITLE **Wave-Mud interactions across the Louisiana Inner Shelf to the Shoreline** | | 5a. CONTRACT NUMBER | |
| | | 5b. GRANT NUMBER | |
| | | 5c. PROGRAM ELEMENT NUMBER | |
| 6. AUTHOR(S) | | 5d. PROJECT NUMBER | |
| | | 5e. TASK NUMBER | |
| | | 5f. WORK UNIT NUMBER | |
| 7. PERFORMING ORGANIZATION NAME(S) AND ADDRESS(ES) **Theiss Research La Jolla, California 92037** | | 8. PERFORMING ORGANIZATION REPORT NUMBER | |
| 9. SPONSORING/MONITORING AGENCY NAME(S) AND ADDRESS(ES) | | 10. SPONSOR/MONITOR'S ACRONYM(S) | |
| | | 11. SPONSOR/MONITOR'S REPORT NUMBER(S) | |
| 12. DISTRIBUTION/AVAILABILITY STATEMENT **Approved for public release, distribution unlimited** | | | |
| 13. SUPPLEMENTARY NOTES **The original document contains color images.** | | | |
| 14. ABSTRACT | | | |
| 15. SUBJECT TERMS | | | |

| 16. SECURITY CLASSIFICATION OF: | | | 17. LIMITATION OF ABSTRACT **SAR** | 18. NUMBER OF PAGES **10** | 19a. NAME OF RESPONSIBLE PERSON |
|---|---|---|---|---|---|
| a. REPORT **unclassified** | b. ABSTRACT **unclassified** | c. THIS PAGE **unclassified** | | | |
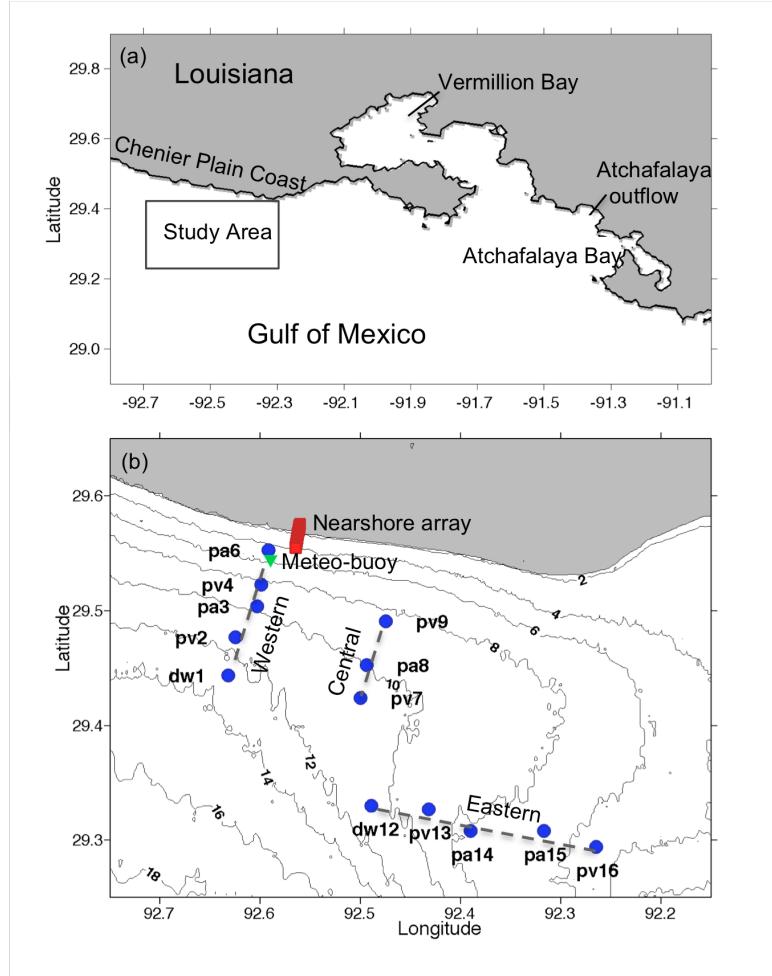
*Figure 1. (a) The study area is located west of the Atchafalaya-Vermillion Bay system in the Gulf of Mexico. (b) Bathymetry (black curves are isobaths, units m) and sensor locations. Blue dots are the inner shelf stations where dw-stations are Datawell Directional Waverider buoys, the pv are Nortek Vector ADV-pressure sensors, and pa are pressure sensors. The nearshore array of SONTEK Triton ADV-pressure sensors is indicated with red squares. The green triangle shows the location of the meteorological buoy.*

**WORK COMPLETED**

## Combining the 2008 MURI data sets

The datasets collected by the NPS/SIO and WHOI teams during the 2008 MURI field experiment on the Louisiana shelf (see also Trainor, 2009; Trainor et al. 2008; Garcia-Garcia et al, 2012), were combined into a comprehensive dataset. The combined data set includes a three-transect array on the inner shelf (Figure 1, inset 1) and a high-resolution nearshore array that smoothly connects to the shallow-end of the western transect of the shelf array (Figure 1, inset 2). The new data set includes observations with a high spatial resolution (see figure 2) across many wavelengths (approximately 25 km) and will provide a much-needed database for the study of the evolution of waves over mud. The dataset consists of observations of a wide range of wave and wind conditions (figure 3), including fetch-limited wave growth (wind from northerly directions), swell propagation (southerly waves, weak winds), and mixed sea-swell events.
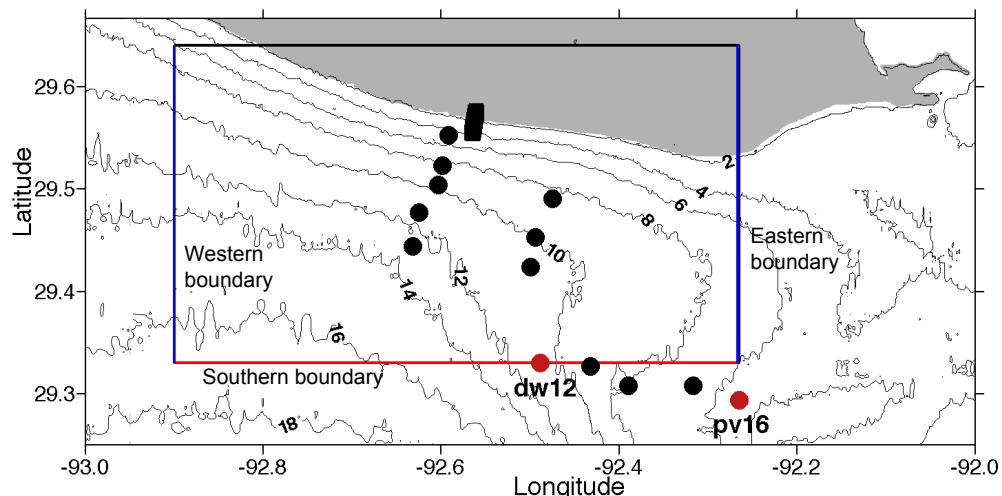


Figure 2 Boundary conditions for the southern boundary (red line) were taken from observations (dw12 and pv16). 1D non-stationary runs, initiated by dw12 and pv16 for the western and eastern boundary (blue lines), respectively, were used as side-boundaries.

## Implementation third-generation wave model

To study the effects of mud on the seafloor on the nearshore wave energy balance in more detail, we have implemented a conventional third-generation wind-wave model (SWAN). Wave boundary conditions are taken from the most offshore buoy (DW12), wind forcing is obtained from meteorological observations made available by the WHOI team (Drs Trowbridge and Fredericks), and bathymetry information was taken from the NOS coastal relief model augmented with nearshore observations by the WHOI team (Elgar 2009, personal communication) during the experiment.

To account for the down-wind variability of the atmospheric boundary layer due to the decrease in roughness length over water, wind speeds during offshore wind events (defined as wind events with

mean wind directions < $\pm\dfrac{\pi}{2}$ from exactly offshore) are modified by a spatially varying scaling factor (Taylor & Lee, 1984). The model was run in third-generation mode (GEN 3) with saturation-based whitecapping (Van der Westhuysen et al., 2007) combined with the Yan wind input term (Yan, 1987). All available source terms are included in the computations except the triad interactions.

The present model implementation was used as a reference for an equivalent sandy shelf to identify the principal effects of the mud on the observed wave dynamics. Thereto we ran the model with a standard bottom friction term (Hasselmann et al., 1973) with the (fixed) friction coefficient set to 0.038 $m^2s^{-3}$ (Van Vledder et al. 2011).

## Analysis of cross-shelf wave dissipation

To analyze the effects of mud on the wave energy balance, we defined a cross-shore direction at about $10^o$ clockwise from North (see figure 2), and assumed straight and parallel depth contours in the alongshore direction so that, for a stationary wave field, the wave energy balance reduces to

$$\frac{d}{dx}\mathcal{F}(\omega,\theta) = \mathcal{S}_{\mathrm{gen}}(\omega,\theta) + \mathcal{S}_{\mathrm{dis}}(\omega,\theta) + \mathcal{S}_{\mathrm{nl}}(\omega,\theta) \tag{1}$$

where $\mathcal{F}(\omega,\theta)$ is the cross-shore wave energy flux and the forcing terms on the right account for (from left to right): wind generation (input), dissipation (whitecapping, wave-bottom interaction etc.), and nonlinear interactions (redistribution). Through comparison of the observed and modeled cross-shore energy flux gradient (1), and normalized growth rate, we assessed the macro-scale effects of wave-mud interaction on evolution of waves across a muddy continental shelf.

We have further considered effects of the nearby Atchafalaya Bay system and the sediment plume dynamics in the coastal zone on the observed wave damping and development.

# RESULTS

The model-data comparison shows that wave heights are generally predicted well with the standard Jonswap bottom friction term, apart from episodic events when dissipation levels in the observations appear to be enhanced (see figure 3). This suggests that a simple (fixed) friction coefficient is inadequate to capture the more dynamic (and time varying) rheology of the muddy seafloor, which is consistent with previous findings by other researchers (e.g. Sheremet et al., 2005). Further, during swell-type events (longer-period waves) the muddy seafloor appears to affect wave-bottom interaction, and results in time-varying enhancement of losses of wave energy. During times that the wind is blowing in offshore direction (fetch-limited and slanted fetch wave growth) the effect of mud appears to be a suppression of wave growth, either through the damping of short waves or through decreasing the effectiveness of the momentum transfer from the wind to the water.
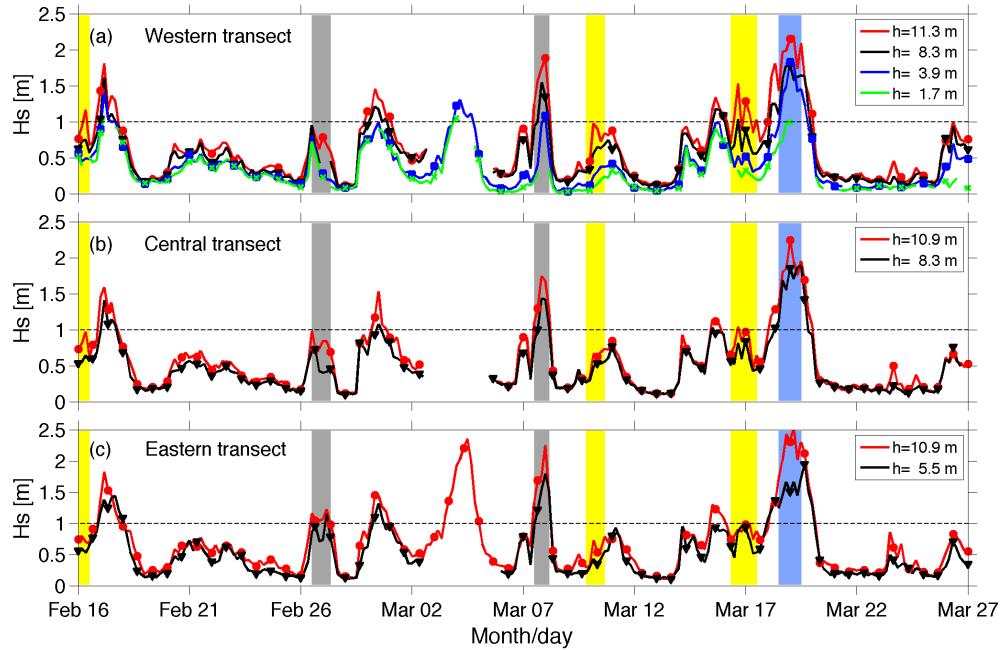


Figure 3. Significant wave height versus time across (a) the western transect in 11.3- (pv2, red curve), 8.3-(pv4, black), 3.9- (n15, blue), and 1.7-m (n4, green) water depths, (b) the central transect in 10.9- (pv7, red) and 8.3-m (pv9, black) water depths, and (c) the eastern transect in 10.9- (dw12, red) and 5.5-m (pv16, black) water depths. The dashed black lines at 1m height are for reference. Data gaps for shelf stations between March 2 and March 5 are due to instrument maintenance. Shaded areas refer to events discussed in the text and indicate periods with large spatial wave variability and strong (> 9 m/s) winds from the northeast (yellow, 0 < dir < 80 deg) and northwest (gray, 300 < dir < 360 deg), as well as a period of large swell (blue).

The model hindcasts are in fairly good agreement with the observed wave height variability during the experiment for all stations. However, for fetch-limited conditions (northerly winds), the model tends to overestimate wave heights (figure 4b), whereas during onshore wave propagation (southerly winds), the agreement is considerably better (figure 4a).
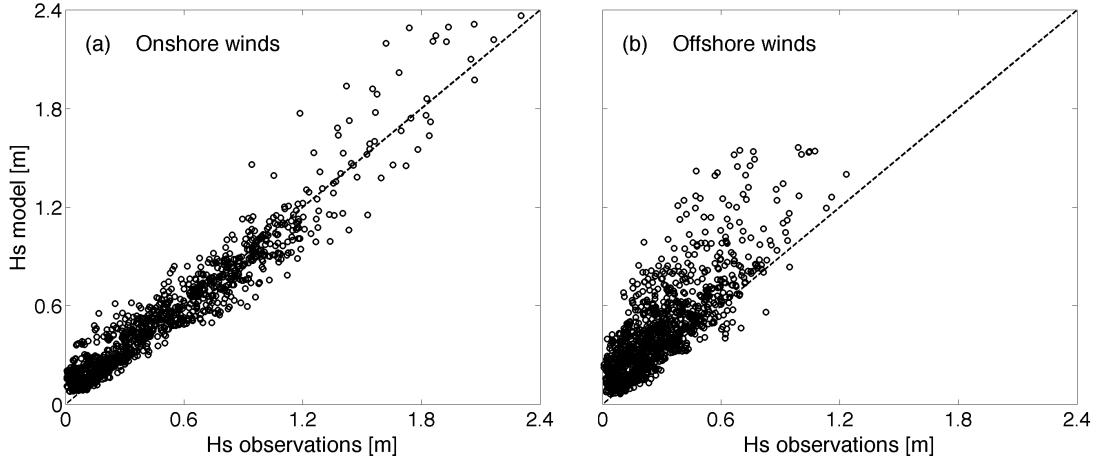
Figure 4. Modeled versus observed significant wave height for all stations on the western and central transects for (a) onshore winds (130°-250° true north) and (b) offshore winds (310° -70°). (Cross-shore is rotated 10° clockwise from true north). The dashed black lines indicate perfect agreement. The slope of the best-fit line is 0.94 for (a) and 1.18 for (b), $r^2$ = 0.94 for (a) and $r^2$ =0.71 for (b), and the root mean square error is 0.11 m for (a) and 0.19 m for (b).

To investigate a possible correlation of coastal sediment plume dynamics with the observed differences in modeled and observed wave growth at higher frequencies, satellite images from MODIS Terra 250 were analyzed. The images were obtained from the NASA EOS Data Gateway, processed with HDFLook, and converted from percentage reflectance to an estimate of total suspended matter in the surface layer (Miller and McKee, 2004).

From the available satellite data (cloud cover limits visibility), it is seen (see e.g. figure 5) that the westward extent of the plume is pushed farther west during easterly wind conditions, resulting in higher surface sediment concentrations at the experiment site. When wind-driven currents carry higher sediment concentrations westward, wave growth owing to winds appears to be suppressed. In contrast, sediment concentrations are relatively low at the experiment site (e.g. March 8 (not shown), and February 28, figure 5c) when modeled and observed wave evolution are in better agreement, including in the higher-frequency energy balance. Moreover, satellite imagery (not shown) suggests that the location of the western sensor transect often coincides with the maximum western extent of the Atchafalaya sediment plume on the shelf (the plume extends farther westward closer to shore). In addition, the western transect also corresponds to the western most extent of Atchafalaya sediment deposition on the shelf (Draut et al. 2005), possibly explaining the rapid "cleaning" of the surface waters in the study area during westerly winds, and therefore the sensitivity to changes in the wind direction in the model-data comparisons.
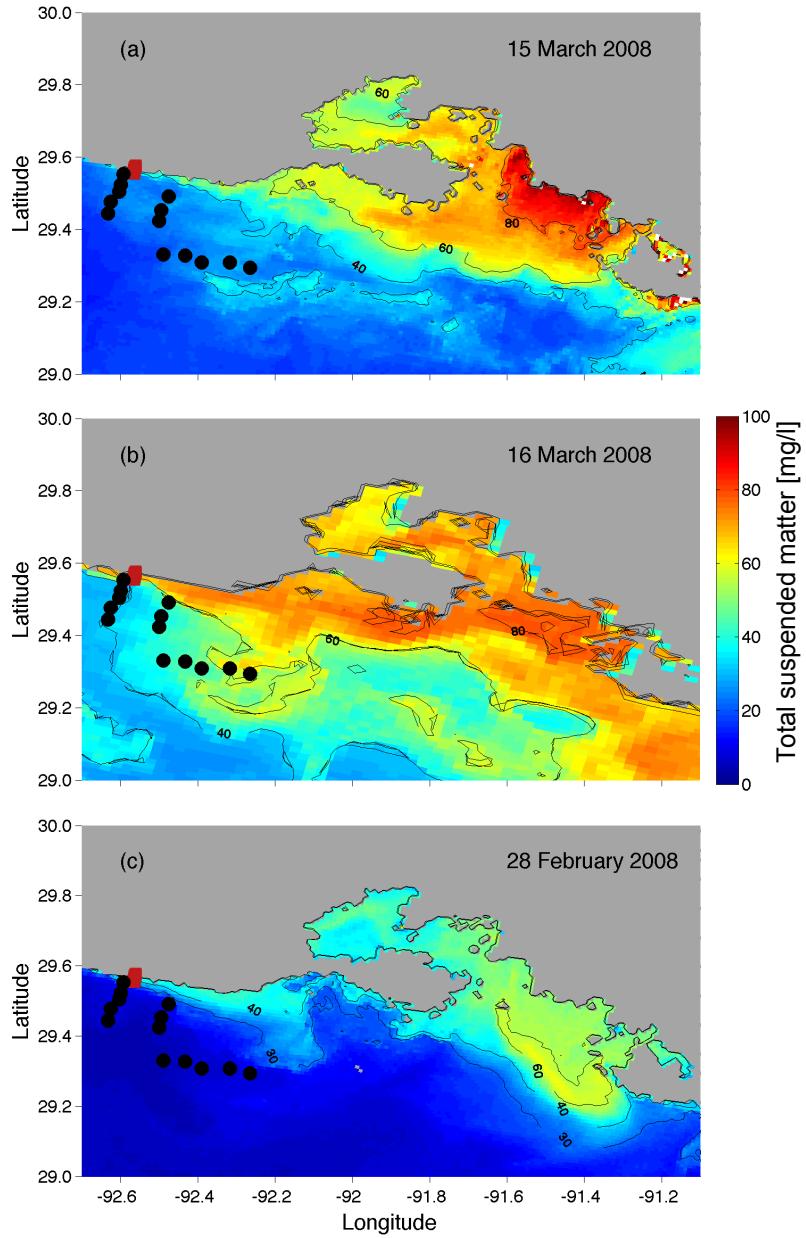
Figure 5. Estimate of total suspended-matter concentrations (from Modis 250 imagery) on (a) March 15, (b) March 16, and (c) February 28. All images were recorded around 17:00 o'clock GMT. High concentrations are red, low concentrations are blue (color scale on right). Grey shading is land. Instrument locations are shown with black circles (shelf stations) and red squares (shoreward stations).

The frequency distribution of the dissipation (see figure 6) between observations and model shows good agreement, although the model underestimates dissipation toward higher frequencies (> 0.2 Hz) at the inner shelf stations. It can be seen (figure 6) that dissipation takes place in the energetic ranges of the spectrum. The distribution of dissipation is mostly consistent with a direct interaction mechanism where damping is induced through interaction of wave-induced fluid motions with the seafloor, such as is the case for bottom friction (Hasselmann et al, 1973), or a direct-interaction two-layer model (e.g.Dalrymple & Liu, 1978; Ng, 2000).

Á
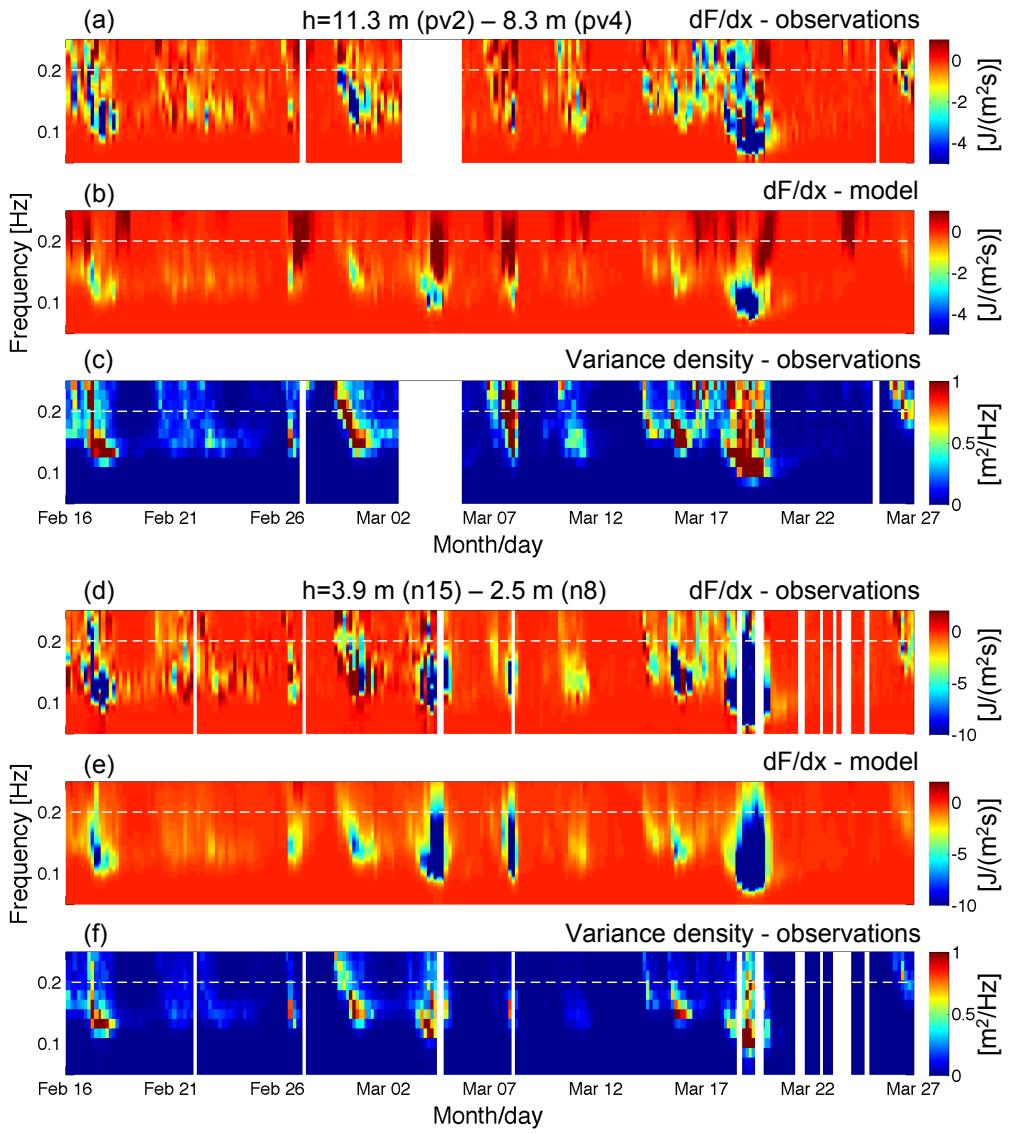
Figure 6. Contours (color scales on the right) of (a and d) observed energy flux gradients, (b and e) modeled (SWAN) energy flux gradients, and (c and f) observed energy density as a function of frequency and time. a-c are between 11.3 and 8.9 m depth and d-f are between 3.9 and 2.5 m depth. Positive flux gradients indicate generation, negative flux gradients indicate dissipation. Note the different scales of (a) and (b) versus (d) and (e).

8

## IMPACT/APPLICATIONS

The availability and analysis of a comprehensive community dataset of wave propagation across a muddy shelf will be an important contribution to the study of wave-mud interactions and the validation and calibration of new theories and modeling approaches.

The fact that the time-varying properties of mud are important even for the macro-scale effects of wave propagation in coastal areas, and cannot be adequately represented by a fixed rheology, is important for operational wave prediction in coastal areas.

## REFERENCES

Dalrymple, R.A., Liu, P. L.-F., 1978. Waves Over Soft Muds: A Two-Layer Fluid Model. Journal of Physical Oceanography, 8, 1121-1131.

Garcia-Garcia, A., T. T. Janssen, T. H. C. Herbers, D. Alden, A. Orange, D. Orange, P. Jessen, S. Kawamoto, and P. Harvey 2012 Sediment Characteristics and paleochannels of the Chenier Plain Inner Shelf, Louisiana, *submitted to Geo-Mar*. Lett.

Hasselmann, K., et al. 1973. Measurements of wind-wave growth and swell decay during the Joint North Sea Wave Project (JONSWAP). *Dtsch. Hydrogr. Z. Sup.* **A8**(12)*,* 95.

Ng, C. 2000 Water waves over a muddy bed: a two-layer Stokes' boundary layer model, *Coast. Engn* **40**, 221-242.

Sheremet, A., Mehta, A. J., Liu, B., Stone, G. W. 2005. Wave–sediment interaction on a muddy inner shelf during Hurricane Claudette. Estuarine,  Coastal and Shelf Science, 63(1-2), 225–233.

Taylor, P.A. and R. J. Lee, 1984 Simple guidelines for wind speed variations due to small-scale topographic features *Clim. Bull.* 1**8**, 3-32

Trainor, L.T., 2009 Field observations and SWAN model predictions of wave evolution in a muddy coastal environment, *MSc dissertation*, Naval Postgraduate School, Monterey 73p.

Trainor, L.T., T.H.C. Herbers, T.T. Janssen, A. Garcia-Garcia, and P.F. Jessen 2008 Observations of ocean surface wave damping on a muddy continental shelf -Louisiana MUDEX 2008, poster presented at AGU meeting, San Francisco

Van der Westhuysen, A.J., M. Zijlema, J.A. Battjes, 2007. Nonlinear saturation-based whitecapping dissipation in SWAN for deep and shallow water. Coastal Engineering 54 (2), 151–170.

Van Vledder, G.,M. Zijlema, L. Holthuijsen, 2010. Revisiting the JONSWAP bottom friction formulation. Proceedings Of The International Conference On Coastal Engineering, 1(32).

## PUBLICATIONS

Engelstad, A., T.T. Janssen, T.H.C. Herbers, G. Ph. Van Vledder, S. Elgar, B. Raubenheimer, L.T. Trainor, and A. Garcia-Garcia, Wave evolution across the Louisiana shelf, *Cont. Shelf Res.*, 2012 [submitted, refereed]